ISSN: 0067-2904

Sensing Properties Of WO_3 /Pd Thin Films Deposited On Porous Silicon Substrates Using Pulsed Laser Deposition

Mayada A. Abed , Falah A-H. Mutlak*
Department of Physics-College of Science, University of Baghdad, Baghdad, Iraq

Received: 29/11/2023 Accepted: 10/7/2024 Published: 15/2/2025

Abstract

The current research examines the distinct sensitivity displayed by WO_3/Pd films prepared using the Pulsed Laser Deposition (PLD technique using a porous silicon substrate (PS). Tungsten oxide impregnated with palladium (WO_3/Pd) films are created for the purpose of sensing Nitrogen Dioxide (NO_2) by employing PLD with different laser pulse energies of 600, 800, and 100 mJ). The ablation process utilizes a laser device that uses a Q-switched Nd:YAG crystal to produce high-intensity light pulses that are precisely 1064 nm in wavelength. A frequency of 1 Hz and a pulse duration of 10 ns characterise the laser system. It operates upon an n-type Si (111) substrate made of porous silicon. Field emission-scanning electron microscopy, photoluminescence spectroscopy, X-ray diffraction, and Raman scattering are used to examine the morphological features, optical structure, and crystal structure of the WO_3/Pd NPs. When the pulse laser's power grows, the WO_3/Pd thin film has sharper peaks, suggesting a strengthening of the crystallinity. The size of the surface grains increased, and this prompted a corresponding increase in the energy gap. As a result, the level of homogeneity was enhanced. The study examines how Pd affects the rate at which nanoparticles of tungsten trioxide grow. A more sensitive response is observed when Pd was present, decrease the operating temperature of the nanoparticles, and keep the sensitivity high even when the temperature is room temperature.

Keywords: Gas sensor; Tungsten trioxide; Palladium; Pulsed Laser Deposition; Porous silicon; Nitrogen Dioxide.

الخصائص التحسسية لأفلام *WO_3 /Pd* على ركيزة السيليكون المسامي باستخدام الترسيب بالليزر النبضي

ميادة عباس عبد, فلاح عبد الحسن مطلك
جامعة بغداد , كلية العلوم , قسم الفيزياء, بغداد, العراق

الخلاصة

يركز البحث الحالي في الحساسية المميزة التي تظهرها أفلام WO_3/Pd التي تم إنشاؤها باستخدام PLD ، أو ترسب الليزر النبضي ، باستخدام ركيزة السيليكون المسامية (PS). تم إنشاء أكسيد التنغستن مع أفلام البلاديوم (WO_3/Pd) بشكل مختبري لاستشعار ثاني أكسيد النيتروجين (NO_2) من خلال استخدام ترسب الليزر النبضي مع شدة نبضة ليزر مختلفة (0.6 ، 0.8 ، و J1). تستخدم عملية الاجتثاث جهازً ليزر Q- switched Nd:YAG لإنتاج نبضات ضوئية عالية الكثافة. 1064 نانومتر في الطول الموجي. مميزات

*Email:falah.mutlak5@gmail.com

نظام الليزر, التردد 1 هرتز ومدة نبضه 10 نانو ثانية. وهي تعمل على ركيزة (N–type Si (111 مصنوعة من السيليكون المسامي. يتم استخدام المجهر الإلكتروني ، التحليل الطيفي للضوء ، حيود الأشعة السينية ، واستطارة رامان لفحص الميزات المورفولوجية ، والبنية البصرية ، والبنية البلورية لـ WO_3/ Pd NPs. عندما تزداد قوة نبضة الليزر ، يكون للفيلم الرقيق WO_3/Pd قممًا أكثر وضوحًا ، مما يشير إلى تعزيز البلورة. زاد حجم الحبوب السطحية ، وهذا ما دفع زيادة مماثلة في فجوة الطاقة. نتيجة لذلك ، تم تعزيز مستوى التجانس. اثبتت الدراسة كيف يؤثر Pd على المعدل الذي تنمو به الجسيمات النانوية من ثالث أكسيد التنغستن. وقد لوحظ استجابة أكثر حساسية عند وجود Pd ، مما يقلل من درجة حرارة التشغيل للجسيمات النانوية ، والحفاظ على الحساسية عالية حتى في درجة حرارة الغرفة.

1. Introduction

Nanomaterials serve as fundamental building blocks within the fields of nanoscience and nanotechnology. The nanostructure science and technology field has had significant global growth in recent years, encompassing a wide range of interdisciplinary research and development endeavours. This technology revolutionized the methodologies employed in creating materials and goods, and expanded the scope and characteristics of functionalities that can be utilized. The commercial impacts of this phenomenon are already substantial and are expected to escalate further [1-5].

Metal oxide semiconductor (MOS) nanostructures are commonly selected for integration into sensors because of their remarkable inherent properties [6-9]. MOS-based chemical sensors have become a highly promising technology for the development of sensor devices. Their compact size, affordability, energy efficiency, real-time operation, microelectronic processing compatibility, nanotechnology integration, and portable device technology are the primary factors contributing to their popularity [9,10].

Tungsten trioxide (WO_3) is categorized as a semiconductor with a large energy band gap [11 -15]. It is a fascinating substance among transition metal oxides; it exhibits a wide array of distinctive characteristics, especially in thin film form, that render it extremely valuable for advanced technological purposes. The material demonstrates structural changes and substoichiometric phase transitions, which have garnered the interest of researchers in recent years in investigating its potential scientific and technological uses in display systems and microelectronics. WO_3 is extensively investigated as an electrochromic material, mainly in its amorphous state. The optical properties of crystalline WO_3 exhibit a significant variation throughout a wide spectrum of wavelengths in both the visible and infrared spectra. Tungsten trioxide can be used as a gas sensor. Being an n-type semiconductor, the sensor's resistance diminishes when it comes into contact with reducing agents, whereas it increases when exposed to oxidizing species. The WO_3 sensor exhibits a notable sensitivity towards many gases, including O_3, O_2, NO_2, NO, NH_3, H_2S, H_2, and ethanol [16-22]. Nevertheless, the electrical characteristics and, consequently, the efficacy of the sensor are significantly influenced by the microstructure of WO_3 nanoparticles. Hence, it is desirable to carefully select the preparation conditions to achieve regulated development and a stable microstructure that can withstand certain gas compositions and temperature ranges [23].

The pulsed laser deposition (PLD) technique is a highly precise method for physical deposition with specific specifications employed in fabricating thin films, which exhibit significant versatility in many materials and applications. The targeted substance is effectively eliminated through the process of ablation, which requires the utilization of a pulsed laser. The laser is frequently utilized at ultraviolet (UV) wavelengths and is employed within a regulated

environment characterized by high-vacuum conditions [24-37]. Xu et al. [38] used the hydrothermal technique to synthesize micro-level WO_3 powder. Cheng et al. [39] used a template-based approach to synthesize WO_3 nanotubes. Doping tungsten trioxide or combining it with other metals yields diverse characteristics, distinct morphological structures, and numerous practical applications [40]. Metal nanoparticles, specifically silver, gold and palladium nanoparticles, have garnered significant interest owing to their distinctive features [41].

The present study involves the fabrication of gas sensors utilising a WO_3/Pd (palladium) composite employing the PLD method (using different laser pulse energies of 600, 800, and 1000 mJ). deposited on porous silicon (PS) substrates. WO_3/Pd (palladium) composite. Surface morphology, optical properties, and crystallinity of the synthetic target were studied using different techniques, including X-ray diffraction (XRD), photoluminescence (PL), field emission scanning electron microscopy (FESEM) and Raman spectroscopy.

2. Material experimental details

Pd and WO_3 powders (supplied from Sigma Aldrich) of 99.9% purity were compressed into three centimetres diameter pellets with a hydraulic press (type SPE CAC), which served as the target. In order to form a high-quality deposit, this project aimed to achieve a significant degree of uniformity and density. Three primary procedures made up the target synthesis process. Photoelectrochemical etching (PECE) refers to a meticulously regulated method wherein material is selectively eliminated on the surface through a synergistic interplay involving electrochemistry processes with light [42, 43]. An n-type porous silicon (100) substrate was effectively coated with thin layers of tungsten trioxide and palladium (WO_3/Pd) using the pulsed laser deposition technique.

A silicon wafer was cut into 1.5×1.5 cm^2 pieces; its resistivity was between 0.1 and 100 Ω cm. The pieces were dried through exposure to ambient air, after which they were cleaned in a mixture of hydrofluoric acid (HF) and ethanol of 2:1 ratio. The specimens were etched with a 532 nm diode laser for 12 minutes, and the current density was 20 mA/cm^2. The electrolyte etching solution was a mixture of 99 per cent ethanol and 48 per cent hydrofluoric acid. Anodization etching was done in Teflon cells, which are well-known for their remarkable resistance to hydrofluoric acid (HF). WO_3 nanoparticles were produced using the laser pulsed deposition (PLD) technique employing a Nd: YAG laser. The target was ablated with a 1064 nm laser of different pulse energies of (0.6, 0.8, and 1) mJ. The number of pulses was 300 pulse; the shot rate of the guns was one hertz. A secondary ablation process using a palladium (Pd) plate was done to ensure that all the targets were getting the same amount of energy. The synthesis of WO_3/Pd was achieved by applying this approach. Referring to JCPDS card No. 96-90-2222, an X-ray diffractometer (Philips PW1050) was used for the X-ray diffraction analyses. A lattice constant of 1.54 Å is associated with Cu-kα. Photoluminescence emission spectra from 200 to 1800 cm^{-1} over a wavelength range of 500 to 700 nm were captured with a fluorescence spectrophotometer.

3. Results and discussion

3.1 Optical characteristics

Photoluminescence spectroscopy at a wavelength of 1064 nm was used to assess the optical properties of WO_3/Pd thin films grown on a PS substrate by PLD technique using different laser pulse energies. The optical properties were considerably affected by changes in the formation conditions, specifically in the presence of porous silicon. This phenomenon was detected during the process of silicon texturing, which involves the use of laser ablation to

induce a transition from a two-electron to a four-electron reaction. As a result, the process of oxide synthesis occurs. It can be noted from the figure that a blue shift in the spectrum occurred as a result of the rise in laser pulse energy which is proportional to the whole width at half maximum (full width at half maximum) reduction. This behaviour aligns with morphological changes consistent with the quantum confinement paradigm. From the PL spectra of WO_3/Pd thin films, band gap energies were measured to be 2.07 eV at 599 nm, 2.10 eV at 589 nm, and 2.13 eV at 581 nm for pulse laser energies of 600, 800, and 1000 mJ, respectively.

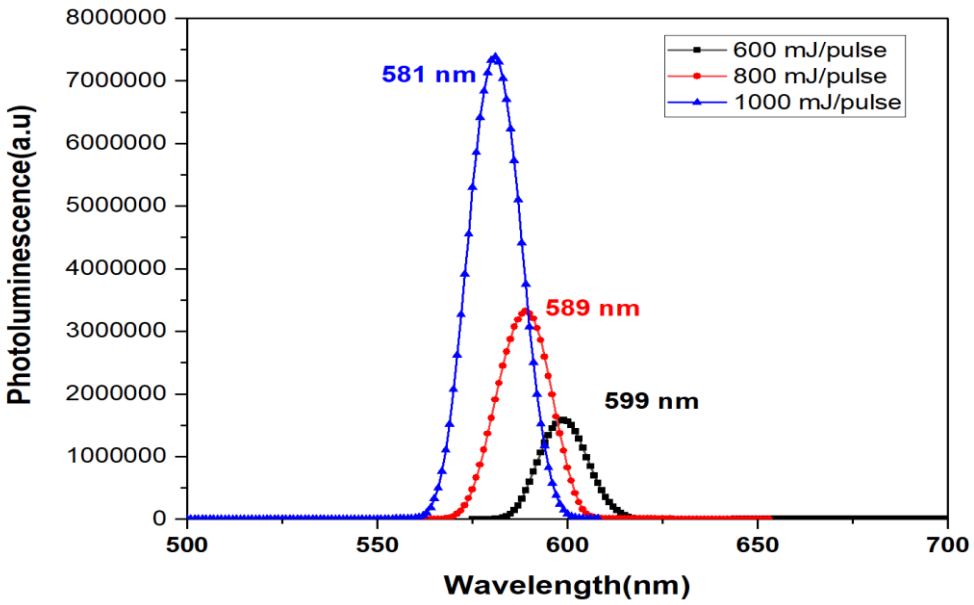

Figure 1: WO_3/Pd thin films PL spectra at varying laser pulse energies at 1064 nm wavelength.

3.2 The vibrational properties

As illustrated in Figure 2, the WO_3/Pd thin films were examined using Raman spectroscopy that fall within 200–1800 cm^{-1}. The dominant peak at a phonon mode of PS has a wavenumber of 519 cm^{-1}. It can be seen in the spectra that there are clear peaks that point to WO_3 having a monoclinic shape. The anti-symmetric stretching of tungsten-oxygen-tungsten (W-O-W) bonds is responsible for the highest point, which was at 804 cm^{-1}. Conversely, the stretching of tungsten-oxygen (W_2O_6 and W_3O_8) bonds shows up as a peak at 710 cm^{-1}. The stretching phase is at 960 cm^{-1} of the terminal W-O bond [44]. The peak that was detected at 260 cm^{-1} results from bending vibrations caused by W-O-W bonds [45,46]. Pd can be identified by three peaks detected at 1248, 1388, and 1572 cm^{-1} [47]. The variation in peak intensity of the spectra is a result of the laser pulse energy changes. The films' spectral characteristics were altered by increasing the laser pulse energy, which improved the Raman bands' efficiency and resolution. Evolution, as we can see, causes changes to peak bands improving their efficiency and specificity. There is more crystallinity when there are clearly defined peaks. Strength and the ability of the bands to distinguish themselves were enhanced. By examining the dataset for prominent peaks, it is possible to deduce the identification of crystalline forms.

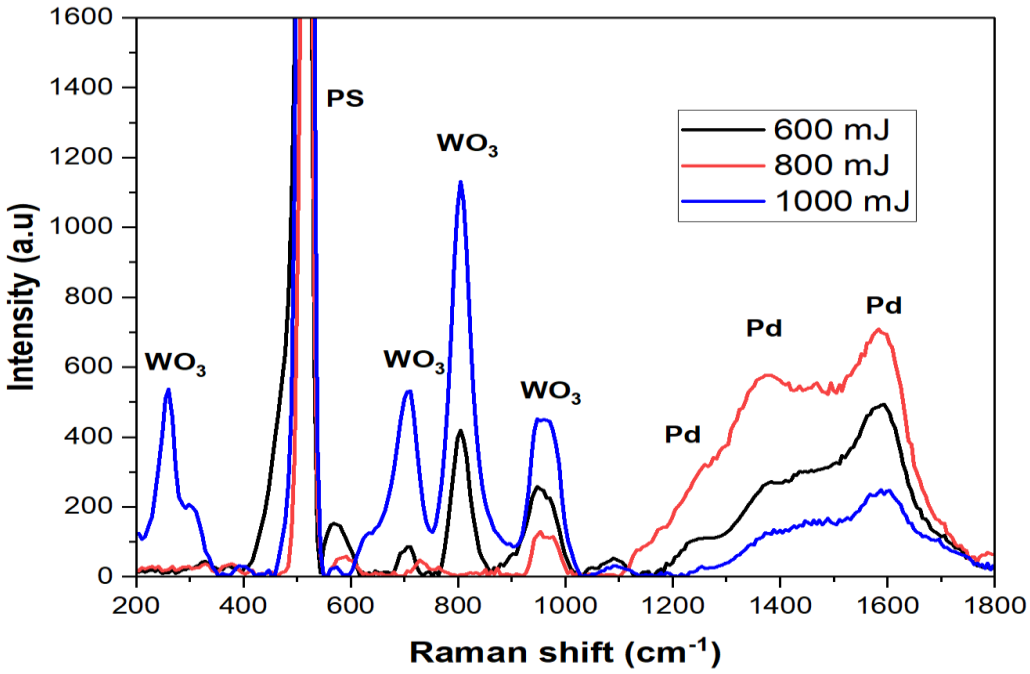

Figure 2: Raman spectra of WO_3/Pd thin film deposited on PS at different Nd:YAG laser pulse energy.

3.3 Microstructural properties

Using the pulsed laser deposition technique, the n-type porous silicon (100) substrate was effectively coated with thin layers of tungsten trioxide and palladium (WO3/Pd). An analysis of the thin film X-ray diffraction pattern (XRD) composed of (WO_3) at different levels of laser energy is illustrated in Figure 3. The 2θ values display high level of conformity with the accepted standard (ICDD No. 96-101-0619). Crystalline levels at (002), (020), (200), (111), and (202) appeared for 2θ angles of 23°, 23.4°, 24°, 26°, and 33°, respectively, indicating a triclinic phase of WO_3.

Results derived from the PS XRD pattern demonstrated a distinct peak at (111) crystallographic plane at a 2θ of 28.8°. The XRD pattern illustrates that the highest peak intensity of Pd was detected at a 2θ of 45°. This angle matched the lattice planes that have been indexed as (111). The experimental results indicated a correlation between the observed diffraction peaks, particularly, face-centered cubic (fcc) Pd crystals. This correlation is supported by the (JCPDS card No. 05-068). The results showed that the size and configuration of the particles can be controlled by changing the laser parameters. When the laser pulse energy was increased, the location of the XRD peak did not change, but the maximum peak crystallinity shifted. The films show a clear tendency to form a crystalline structure at high energy levels. The dynamic interplay of energy at the island borders, together with the repulsive contact between these limits is probably the main cause of the observed morphological alterations.

For the purpose of calculating crystallite sizes in WO_3/Pd films, the Scherrer equation was employed [48]:

$$C.S = \frac{0.9\,\lambda}{\beta\, cos\theta} \quad \text{.....} \quad \text{.....(1)}$$

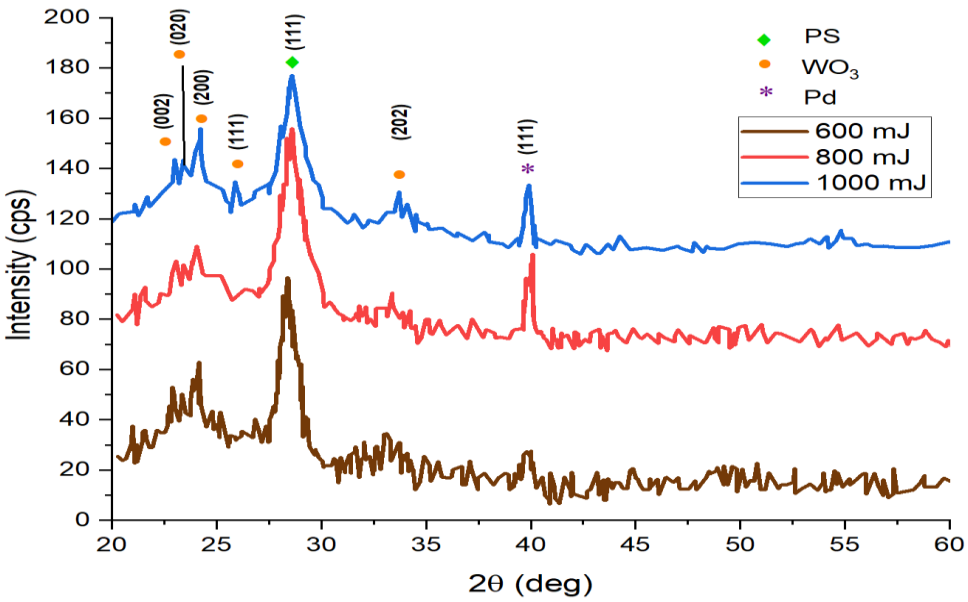

Figure 3: The XRD patterns of a WO_3/Pd thin film prepared using a Nd:YAG laser.

Table 1 analyses the impacts of laser pulse energy on the thin film deposition process. The correlation between the energy of the pulse laser and the size of the crystallites can explain the observed decrease in the Full Width at Half Maximum (FWHM). The study results show a positive correlation between the sample's energy deposition and the particle size distribution. This phenomenon may be associated with an increase in the rate of atomic growth and a partial reduction in particle size. This enhances crystal formation in the sample and reduces crystalline defects [49]. However, a subsequent transition towards a diminished angle of refraction accompanies this decline.

Table 1: XRD results of the Tungsten Trioxide/Palladium (WO_3/Pd) thin films prepared using the PLD technique.

Energy (J/pulse)	2θ (Degree)	hkl	FWHM (rad)	crystal size (nm)	d_{hkl} (Å)
0.6 J	22.9	002	0.00574	26.203	0.038
	23.3	020	0.00556	27.141	0.038
	24.1	200	0.0069	21.8153	0.036
	25.16	111	0.00744	20.522	0.035
	33.1	202	0.008	18.801	0.027
	40	111	0.01009	18.02	0.022
0.8 J	23.07	002	0.0073	20.6412	0.038
	23.42	020	0.0678	22.2781	0.037
	24.07	200	0.0078	19.3763	0.037
	33.37	202	0.0052	31.767	0.026
	40.07	111	0.0078	23.107	0.022
1 J	23	002	0.00365	41.251	0.038
	23.42	020	0.0083	25.4971	0.037
	24.22	200	0.00522	29.5904	0.036
	25.9	111	0.00609	24.5521	0.034
	33.7	202	0.00539	30.765	0.026
	39.9	111	0.0057	31.248	0.022

Figure 4 shows the FE-SEM images of the film's as-deposited surface morphologies. Examining the film's structure uncovered a porous structure with visible black holes or zones on its surface. The small surface fractures in films developed at high laser pulse energy can serve as pathways for gas molecules to enter the film, thereby impacting the performance of the WO_3/Pd sensor.

Grain size uniformity was improved with the increase of the energy pulse, leading to larger surface grains; bigger surface grains could form as neighbouring small crystals combined. Thus, the WO_3/Pd thin films fabricated by PLD at 1000mJ laser energy exhibited the largest size grains; the surface grains ranged in size from 100 to 300 nanometres. The results of a previous study [50], indicated the existence of a surface particle property, as depicted in Figure 4. This implies that the specific arrangement of the WO_3/Pd thin film is expected to enhance NO_2 gas molecules' adsorption process in a gas sensor. The structural features of the film, including its large surface area and small pore diameters, may explain why NO_2 molecules should be able to be adsorbate with relative ease.

Figure 4 also shows the results of analysing the weight percentages of tungsten (W), oxygen (O), and palladium (Pd) in the collected samples at different laser pulse energies. Images from the elemental mapping show that the sample has a very even distribution of W, Pd, and O atoms. Based on the absence of any further peaks that could be linked to impurities, it can be concluded that the WO_3/Pd thin film that was created in this study is of excellent quality.

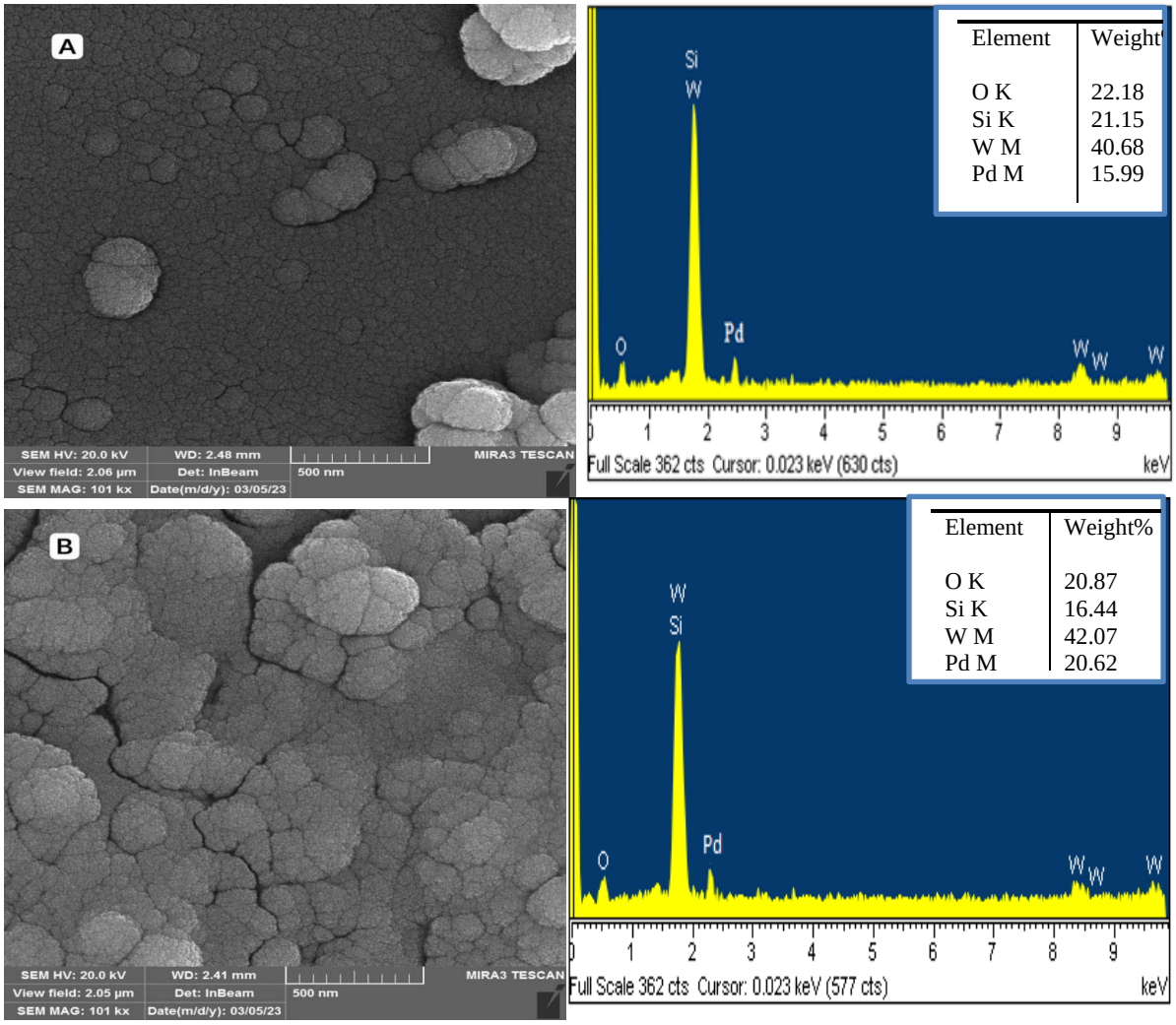

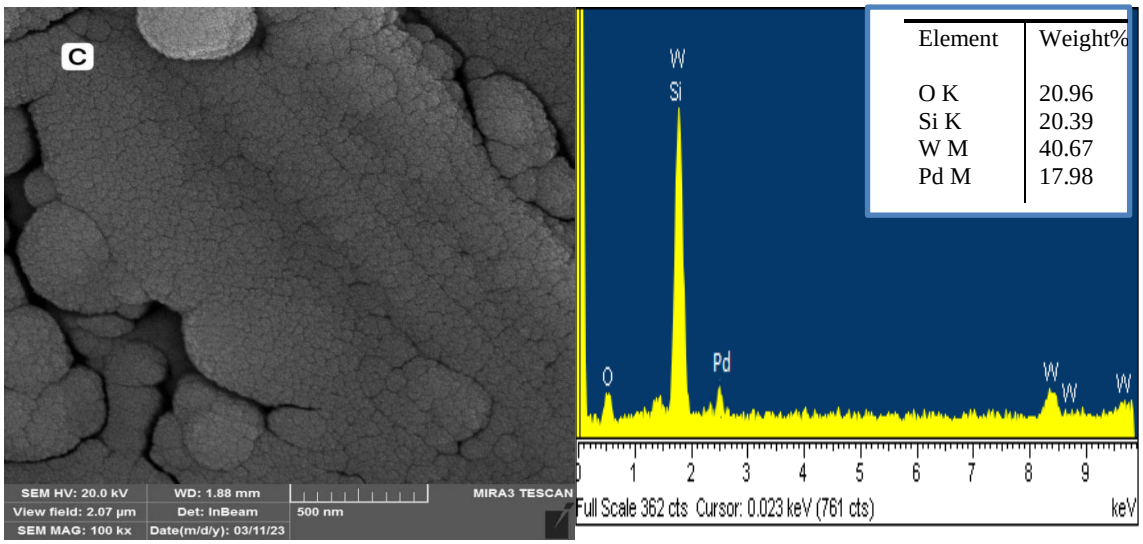

Figure 4: FE-SEM images of WO_3/Pd NPs deposited on PS at (A) 600mJ/pulse, (B) 800 mJ/pulse, and (C) 1000mJ/pulse laser ablated energies.

3.2 Characteristics of nitrogen dioxide (NO_2) sensors

To ensure the precision of the sensing data, the WO_3/Pd thin films were first deposited at room temperature. It was tested as a sensor in the temperature range of 300 to 2500 °C. The films were exposed to gas multiple times to determine how long the film's response would last. The purpose of this is to study the thin film resistance changes with each exposure.

Gas sensing measures take several factors into consideration. The gas detection sensor's parameters include sensitivity, response time, recovery time, with bias voltage of 6 volts. NO_2 gas was produced in the lab. by the reduction of concentrated nitric acid with copperas in the following chemical equation:

$$4HNO_3 + Cu \rightarrow Cu(NO_3)_2 + 2NO_2 + 2H_2O \quad (1)$$

The samples were subjected to temperatures ranging from 30^0 to 250^0 C. The vacuum evaporation process was employed with a thermal coating machine (Edward type 306) to the masks, which utilised porous silicon wafers as the substrate. The masks were of aluminium foil containing 300 nm-thick; aluminium electrodes were utilised in this investigation. The distance between each electrode was precisely 0.5 millimetres. The investigation conducted temperature adjustments on the samples within the specified range of 30°C to 250°C to evaluate the sensitivity, reaction, and recuperation time of the specimen. The experimental setup comprised a 3% NO_2 and 97% air mixture, with a bias voltage of 6 V.

It is typical for ceramic materials to experience a reduction in resistance when exposed to air at high temperatures. It was noted that the sensor's resistance had substantially increased upon exposure to gas introduced into the test chamber, eventually reaching saturation. A significant decrease in the resistance recorded by the sensors was observed after the gas flow was turned off, as shown in Figure 5.

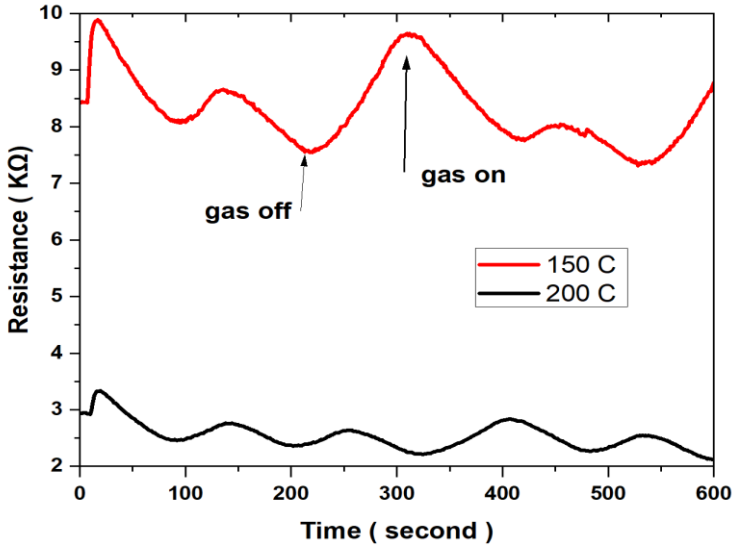

Figure 5: Electrical resistance of WO_3/Pd thin films at different temperatures on exposure to NO_2 gas

The film's sensor response (S) was calculated as the change of the sensor resistance with the test gas on and the gas off at constant operating temperature to its resistance when the test gas is on. This ratio is stated as [51]:

$$S = \frac{R\ on - R\ off}{R\ on} \times 100\% \quad (2)$$

The variable (Ron –Roff) represents the difference in the resistance of the film before and after exposure to the test gas. The variable R represents the initial resistance of the film while it is in an air atmosphere.

The sensitivity of WO_3/Pd sensors to NO_2 gas across a temperature range of 30 to 250 C^0 is shown in Figure 6. It shows a significant sensitivity of WO_3/Pd sensors to NO_2 gas; it can be detected even at very low temperatures, even at room temperature. Detection efficiency peaked at 25.4% at 30°C and 1000mJ of laser pulse energy. However, 48.3% was the highest value seen at 100°C.

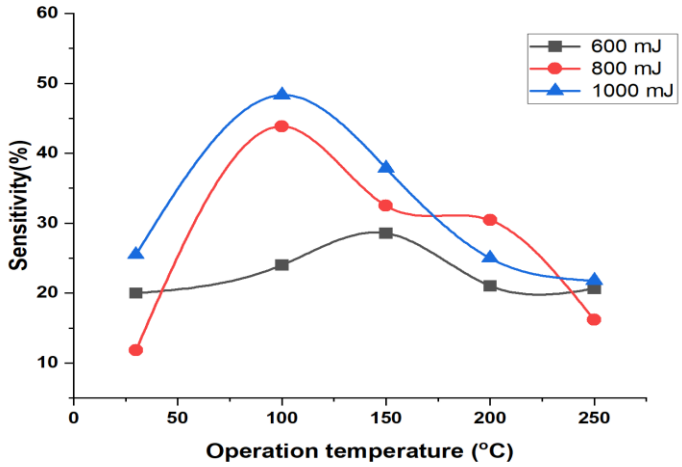

Figure 6: The sensitivity of the WO_3/Pd sensors to NO_2 at different laser pulse energies

The recovery and time-based response times of WO_3/Pd sensors, which are recognized for their exceptional sensitivity to atmospheric NO_2 concentrations, are illustrated in Figure 8.

The response time exhibited a negative correlation with the rise in temperature. It is hypothesized that the longer response times observed at lower temperatures was because the measurement chamber achieved a low partial pressure of NO_2, which can be attributed to its substantial volume. This hypothesis is supported by the validity of the patterns of change in transmittance at both low and high concentrations.

The following equations were used to compute the response and recovery times of the sensor [52]:

$$Response\ time\ =\ |time\ \ gas(on) - time\ gas(off)\ | * 0.9 \ldots..(4)$$

$$Recover\ time\ =\ |time\ gas(off) - time\ gas(recover)\ | * 0.9 \ldots..(5)$$

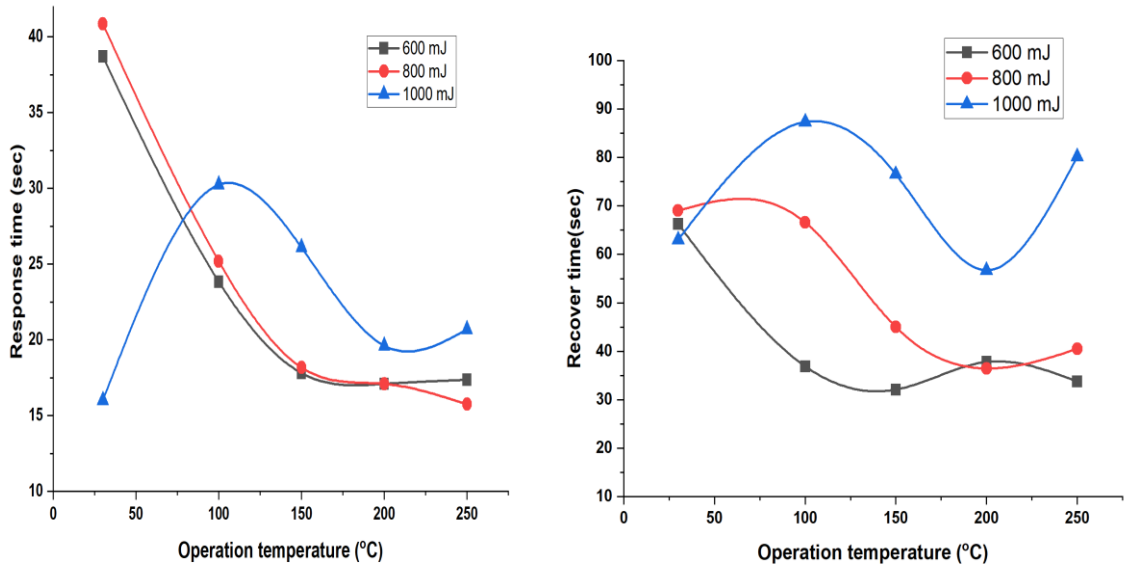

Figure 7: Response time and recovery time of WO_3/Pd sensor prepared by PLD technique and subjected to different laser pulse energies against NO_2 gas

The gas sensor's sensitivity and selectivity can be improved by introducing a metal catalyst (Pd) into the sensor material. Introducing a metal catalyst into a mixture with a metal oxide facilitates the smooth flow of electrons. This electron transfer process results in an enhanced quantity of adsorbed species participating in the adsorption and desorption phenomena. Consequently, this leads to a heightened shift in electrical conductivity. To enhance the efficacy of catalysis, it is imperative to augment the catalyst's surface area that comes into touch with the gas. In addition to affecting sensitivity and selectivity, this enhancement reduces the operating temperature. In a previous study [53], the impact of Pd on the kinetics of WO_3 nanoparticles' growth was investigated, revealing that Pd can enhance sensitivity while concurrently reducing the operational temperature. In addition, the nanoparticles demonstrated significant sensitivity even at room temperature.

A greater number of grain boundaries, or areas with enhanced gas sensitivity, can be induced by increasing the laser pulse energy. Therefore, due to the effects of grain size, sensitivity may rise.

4. Conclusions

In summary, thin films of WO_3/Pd were developed using the pulsed laser deposition technique, a which facilitates the production of amorphous, uniformly textured, and homogenous thin films. The physical characteristics of films are crucial in determining the sensing capabilities of thin film sensors. FE-SEM images revealed that the films possessed a microstructure with pores characterized by small cracks. This microstructural feature enhances the detection reaction due to the strong interaction of gas molecules with the film. The sensitivity may increase as a result of the large grain size. The sensitive nature of the WO_3/Pd deposition of a thin layer was shown to be improved by increasing the laser pulse energy. The Pd layer, serving as a catalyst, was included to enhance the sensor sensitivity to NO_2 gas and reduce its operational temperature. The sensitivity of the sensor to NO_2 gas increased with the increase of the laser pulse energy utilised during the deposition process.

The longer response times reported at lower temperatures are a notable observation. The sensor's high selectivity and sensitivity, rapid response, and swift recovery times are well-suited for gas sensing applications even at low temperatures.

References

[1] D. Nunes, M. Vilarigues, J. B. Correia, and P. A. Carvalho, "Nickel–carbon nanocomposites: Synthesis, structural changes and strengthening mechanisms," Acta materialia, vol. 60, no. 2, pp. 737-747, 2012.

[2] I. Khan, K. Saeed, and I. Khan, "Nanoparticles: Properties, applications and toxicities," *Arabian journal of chemistry*, vol. 12, no. 7, pp. 908-931, 2019.

[3] Q. Zhang, K. Zhang, D. Xu, G. Yang, H. Huang, F. Nie, C. Liu, and S. Yang, "CuO nanostructures: synthesis, characterization, growth mechanisms, fundamental properties, and applications," *Progress in Materials Science*, vol. 60, pp. 208-337, 2014.

[4] M. A. Abed, F. A-H Mutlak, M. S. Jabir, and A. F. Ahmed, "Toxicity analysis of Ag/Au core/shell nanoparticles synthesizes via seed-growth on blood human components," In *AIP Conference Proceedings*, vol. 2372, no. 1, p. 100004, 2021.

[5] H. A. Alrubaie, and B. M. Alshabander, "The effect of ZnO nanoparticles on the self-cleaning of ZnO/epoxy composites," In *AIP Conference Proceedings*, vol. 2437, no. 1. P. 020184, 2022.

[6] M. Tiemann, "Porous metal oxides as gas sensors," *Chemistry–A European Journal*, vol. 13, no. 30, pp. 8376-8388, 2007.

[7] B. Saruhan, R. L. Fomekong, and S. Nahirniak, "Influences of semiconductor metal oxide properties on gas sensing characteristics," *Frontiers in Sensors*, vol. 2, pp. 657931, 2021.

[8] S. Qasim, A. F. AbdulAmeer, and A. H-A Jalaukhan, "Structural and Morphological Properties of As-Deposited and Heat-Treated Blended Graphene Oxide/Poly (3, 4-Ethylenedioxythiophene)-Poly (Styrenesulfonate) Thin Films," *Iraqi Journal of Science*, vol. 62. no. 11, pp. 4416-4424, 2021.

[9] K. G. Krishna, S. Parne, N. Pothukanuri, V. Kathirvelu, S. Gandi, and D. Joshi, "Nanostructured metal oxide semiconductor-based gas sensors: A comprehensive review," *Sensors and Actuators A: Physica,l* vol. 341, p. 113578, 2022.

[10] P. Patial and M. Deshwal, "Selectivity and sensitivity property of metal oxide semiconductor-based gas sensor with dopants variation: A review," *Transactions on Electrical and Electronic Materials*, vol. 23, no. 1, pp. 6-18, 2022.

[11] A. Dey, "Semiconductor metal oxide gas sensors: A review," Materials science and Engineering: B, no. 229, pp. 206-217, 2018.

[12] N. K. Pandey, Karunesh Tiwari, and Akash Roy, "Synthesis and Characterization of WO3 Nanomaterials," *Biomedical Nanotechnology*, vol. 7, no. 1, pp. 156–157, 2011.

[13] E. Comini, G. Faglia, G. Sberveglieri, Z. Pan, and Z. L. Wang, "Stable and highly sensitive gas sensors based on semiconducting oxide nanobelts," *Applied physics letters*, vol. 81, no. 10, pp. 1869-1871, 2002.

[14] O. K. Varghese, and C. A. Grimes, "Metal oxide nanoarchitectures for environmental sensing," *Journal of nanoscience and nanotechnology*, vol. 3, no. 4, pp. 277-293, 2003.

[15] A. Kolmakov, and M. Moskovits, "Chemical sensing and catalysis by one-dimensional metal-oxide nanostructures," *Annu. Rev. Mater. Res.*, vol. 34, pp. 151-180, 2004.

[16] N. Barsan, and U. Weimar, "Understanding the fundamental principles of metal oxide-based gas sensors; the example of CO sensing with SnO2 sensors in the presence of humidity," *Journal of Physics: Condensed Matter*, vol. 15, no. 20, R813, 2003.

[17] C. Cantalini, W. Wlodarski, Y. Li, M. Passacantando, S. Santucci, E. Comini, G. Faglia, "Investigation on the O3 sensitivity properties of WO3 thin films prepared by sol–gel, thermal evaporation and r.f. sputtering techniques," *Sens. Actuators B: Chemical*, vol. 64, no. 1-3, pp.182–188,2000.

[18] K. Galatsis, Y.X. Li, W. Wlodarski, K. Kalantar-Zadeh, "Sol–gel prepared MoO3–WO3 thin-films for O2 gas sensing," *Sens. Actuators B: Chemical*, vol. 77, no. 1-2, pp.478–483, 2001.

[19] D-S. Lee, K-H. Nam, D-D. Lee "Effect of substrate on NO2-sensing properties of WO3 thin film gas sensors," *Thin Solid Films*, vol. 375, no. 1-2, pp. 142–146, 2000.

[20] B. Frühberger, M. Grunze, DJ. Dwyer, "Surface chemistry of H_2S-sensitive tungsten oxide films," *Sens. Actuators B: Chemical*, vol. 31, no. 3, pp. 167–174, 1996.

[21] C. Kamble, M. Panse, and A. Nimbalkar. "Ag decorated WO3 sensor for the detection of sub-ppm level NO2 concentration in air," *Materials Science in Semiconductor Processing*, vol. 103, p. 104613, 2019.

[22] V. Hariharan, B. Gnanavel, R. Sathiyapriya, and V. Aroulmoji. "A review on tungsten oxide (WO3) and their derivatives for sensor applications," *International journal of advanced Science and Engineering*, vol. 5, pp. 1163-1168, 2019.

[23] GN. Chaudhari, AM. Bende, AB. Bodade, SS. Patil, VS. Sapkal. "Structural
and gas sensing properties of nanocrystalline TiO2: WO3 –based hydrogen sensors," Sens. *Actuators B: Chemical*, vol. 115, no. 1, pp. 297–302, 2006.

[24] PJ. Shaver, "Activated tungsten oxide gas detectors," *Appl. Phys. Lett.*, vol. 11, no. 8, pp. 255–257, 1967.

[25] F. A-H. Mutlak, R.K Jamal, A. F. Ahmed, "Pulsed Laser Deposition of TiO2 Nanostructures for Verify the Linear and Non-Linear Optical Characteristics," *Iraqi Journal of Science*, vol. 62, no. 2, pp. 517-525, 2021.

[26] T.M. Rashid, U.M. Nayef, M.S. Jabir, F.A.H. Mutlak, "Study of optical and morphological properties for Au-ZnO nanocomposite prepared by Laser ablation in liquid," *Journal of Physics: Conference Series*, vol. 1795, p. 012041, 2021.

[27] T.M. Rashid, U.M. Nayef, M.S. Jabir, F.A.H. Mutlak, "Synthesis and characterization of Au: ZnO (core: shell) nanoparticles via laser ablation," *optik*, vol. 244, p. 167569, 2021.

[28] D.H. Jwied, U.M. Nayef, F.A.H. Mutlak, "Synthesis of C: Se nanoparticles via laser ablated with magnetic field on porous silicon for gas sensor applications," *optik*, vol. 242, p. 167207, 2021.

[29] QK. Hammad, AN. Ayyash, F.AH. Mutlak. "Improving SERS substrates with Au/Ag-coated Si nanostructures generated by laser ablation synthesis in PVA," *J Opt*, vol. 52, pp. 1528–1536 2023.

[30] F. A.H Mutlak, M. Jaber, H. Emad,"Effect of Laser Pulse Energy on the Characteristics of Au Nanoparticles and Applications in medicine," *Iraqi Journal of Science*, vol. 58, no. 4C, pp. 2364-2369, 2017.

[31] D. E Williams, "Semiconducting oxides as gas-sensitive resistors." Sen. Actuators B., vol. 57, no.1, 1999.

[32] A.S Alber, F. AH. Mutlak. "A novel laser-assisted approach for synthesis of AuNPs/PS nanostructures as photodetector," *Journal of Optics*, vol. 52, no. 3, pp. 1477-1487, 2022.

[33] A. J. Jwar, U. Nayef, F. A.-H. Mutlak, "Study Effect of Magnetic Field on Au-TiO2 Core–Shell Nanoparticles via Laser Ablation Deposited on Porous Silicon for Photodetector," *Plasmonics*, vol. 18, pp. 595-605, 2023.

[34] V.C. Nguyen, HY. Cha, H. Kim. "High Selectivity Hydrogen Gas Sensor Based on WO3/PdAlGaN/GaN HEMTs," *Sensors*, vol. 23, no. 7, p. 3465, 2023.

[35] A F. Ahmed, and A. A. Yousef, "Spectroscopic Analysis of DC-Nitrogen Plasma Produced using Copper Electrodes," *Iraqi Journal of Science*, vol. 62, no. 10, pp. 3560-3569, 2021.

[36] K. A. Aadim, and A. A. Yousef. "Spectroscopic study of AL nitrogen plasma produced by DC glow discharge," *Iraqi Journal of Science*, vol. 59, no. 59, pp. 494-501, 2018.

[37] W. S. Hussein, A. F. Ahmed and K. A. Aadim. "Influence of laser energy and annealing on structural and optical properties of CdS films prepared by laser induced plasma," *Iraqi Journal of Science,* vol. 61, no. 6, pp.1307-1312, 2020

[38] Y. M. Xu, L. H. Huo, H. Zhao, S. Gao, and J. G. Zhao, "Hydrothermal synthesis and Phototropism property of superfine powder of metastable tungsten oxide (in Chinese*)," Chin. J. Inorg. Chem.*, vol. 21, no. 4, pp. 538-541, 2005.

[39] L. F. Cheng, X. T. Zhang, Y. H. Chen, B. Liu, Y. C. Li, Y. B. Huang, and Z. L. Du. "A simple method for synthesizing WO3 nanotubes," *chemical journal of Chinese universities-chinese,* vol. 25, no. 9, pp. 1621-1623, 2004.

[40] W. Qu, R. Green, and M. Austin. "Development of multi-functional sensors in thick-film and thin-film technology," *Measurement Science and Technology,* vol. 11, no. 8, p. 1111, 2000.

[41] Y. Sun, and Y. Xia. "Large-scale synthesis of uniform silver nanowires through a soft, self-seeding, polyol process," *Advanced Materials*, vol. 14, no. 11, pp. 833-837, 2002.

[42] F. A.H. Mutlak, A.B. Taha, U.M. Nayef, "Synthesis and characterization of SnO2 on porous silicon for photoconversion," *Silicon*, vol. 10, no. 3, pp. 967–974, 2017.

[43] M. A. Abed and F. A.-H. Mutlak, "Production and characterization of porous silicon via laser-assisted etching as photodetector: effect of different HF concentrations," *Journal of Optics*, pp. 1-11, 2023.

[44] N.H. Harb, and F. A-H. Mutlak. "Production and characterization of Tungsten Trioxide nanoparticles on porous silicon as photoconductive detector via pulsed laser deposition," *Optik*, vol. 257, pp. 168815, 2022.

[45] A. T. S. A. Jaworek, and A. T. Sobczyk. "Electrospraying route to nanotechnology: An overview," *Journal of electrostatics*, vol. 66, no. 3-4, pp. 197-219, 2008.

[46] B. Pecquenard, H. Lecacheux, J. Livage, C. Julien, "Orthorhombic WO3 formed via
a Ti-stabilized WO3 • 1/3 H2O phase," *J. Solid State Chem.*, vol. 135, no. 1, pp.159–168, 1998.

[47] Q. Chen, M.M. Hassan, J. Xu, M. Zareef, H. Li, Y. Xu, P. Wang, A.A. Agyekum, F.Y.H. Kutsanedzie… "Fast sensing of imidacloprid residue in tea using surface-enhanced Raman scattering by comparative multivariate calibration," *Spectrochim. Acta Part A Mol. Biomol. Spectrosc*. vol. 211, pp. 86–93, 2019.

[48] N. H. Harb "The structure and optical properties of Ag doped CdO thin film prepared by pulse laser deposition (PLD)," *Baghdad Science Journal*, vol. 15, no. 3, pp. 300-303, 2018.

[49] S. N. Rashid, "Comparison Study of The Effect of Thermal Annealing and CO2 Laser Annealing on Structural and Optical Properties of Thin Films Prepared by Sol-Gel Method," M.Sc. thesis, College of sciences, University of Tikrit, (2016).

[50] W. F. Tseng, J. W. Mayer, S. U. Campisano, G. Foti, and E. Rimini. "Grain size dependence in a self-implanted silicon layer on laser irradiation energy density." Applied Physics Letters 32, no. 12, pp. 824-826. (1978).

[51] V. E. Bochenkov and G. B. Sergeev, "Sensitivity, Selectivity and Stability of Gas-Sensitive Metal-Oxide Nanostructures", State American Scientific Publishers, 2010, vol. 3, pp. 31-52.

[52] R. Nisha, "Development of semiconductor metal oxide gas sensors for the detection of NO2 and H2S gases," Ph.D. Thesis, Cochin University of Science and Technology, Cochin, India, 2013.

[53] S Fardindoost, F Rahimi, R Ghasempour ; "Pd doped WO3 films prepared by sol–gel process for hydrogen sensing" ,International Journal of Hydrogen Energy, 35, no. 2, pp.854-860, 2010.